nature climate change

LETTERS

PUBLISHED ONLINE: 11 NOVEMBER 2012 | DOI: 10.1038/NCLIMATE1725

Assessment of groundwater inundation as a consequence of sea-level rise

Kolja Rotzoll[1]* and Charles H. Fletcher[2]

Strong evidence on climate change underscores the need for actions to reduce the impacts of sea-level rise. Global mean sea level may rise 0.18–0.48 m by mid-century[1,2] and 0.5–1.4 m by the end of the century[2]. Besides marine inundation, it is largely unrecognized that low-lying coastal areas may also be vulnerable to groundwater inundation, which is localized coastal-plain flooding due to a rise of the groundwater table with sea level. Measurements of the coastal groundwater elevation and tidal influence in urban Honolulu, Hawaii, allow estimates of the mean water table, which was used to assess vulnerability to groundwater inundation from sea-level rise. We find that 0.6 m of potential sea-level rise causes substantial flooding, and 1 m sea-level rise inundates 10% of a 1-km wide heavily urbanized coastal zone. The flooded area including groundwater inundation is more than twice the area of marine inundation alone. This has consequences for decision-makers, resource managers and urban planners, and may be applicable to many low-lying coastal areas, especially where groundwater withdrawal is not substantial.

Coastal regions with low elevations and dense populations are at the highest risk of marine flooding. Global estimates suggest that more than 20 million people live below normal high-tide levels and more than 200 million people are vulnerable to flooding during temporary sea-level extremes[3]. Areas with a higher elevated shoreline than the hinterland are somewhat protected from marine inundation; however, groundwater inundation is a further risk faced by coastal plains before marine flooding occurs (Fig. 1). The groundwater table in unconfined aquifers typically lies above mean sea level[4], fluctuates with daily tides and other low-frequency sources of ocean energy, and amplitudes decrease exponentially with distance from the shoreline[5]. As sea level rises, the water table will rise simultaneously[6] and eventually break out above the land surface creating new wetlands and expanding others, changing surface drainage, saturating the soil, and inundating the land depending on local topography. Flooding will start sporadically but will be especially intense seasonally when high tide coincides with rainfall events. Rising groundwater levels could cause long-term problems related to water management (aquifer salinization) and infrastructure (flooding) in coastal areas, which could be costly to mitigate even when they are not catastrophic[7]. Thus, groundwater inundation requires a more complex assessment of adaptation tools and strategies than marine inundation alone. This study focuses on southern Oahu, Hawaii; yet the problem is applicable to most low-lying coastal lands where the water table (freshwater or otherwise) is near the surface.

The coastal aquifer in southern Oahu is a complex of sedimentary deposits ranging from variably porous limestone to low-permeability alluvium[8] called 'caprock' (Fig. 1). Although the unconfined caprock aquifer is heterogeneous, it is often treated as a homogeneous unit confining the underlying basalt aquifer, which is the primary drinking-water source on the island[9]. In this study, we compile existing groundwater data to estimate the current water table in the southern Oahu caprock aquifer and assess how potential future SLR could affect inundation potential and timing.

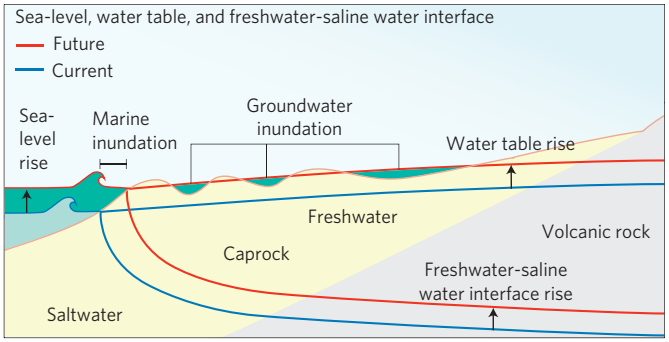

Figure 1 | Conceptual diagram of a freshwater lens, and marine and groundwater inundation under SLR in the southern Oahu aquifer.

Measured tidal efficiencies in the Honolulu and Pearl Harbor caprock aquifer (Fig. 2) show the characteristic exponential decay of amplitude with distance from the boundary (Fig. 3a). At 1 km inland, tidal amplitudes decrease to 1% of ocean amplitude. Scatter in the attenuation plot can be attributed to aquifer heterogeneity at the regional scale, plausible because of the one-dimensional simplification of the study area. The slope of the regression line fitted to observations provides an effective aquifer diffusivity of 1.3×10^5 m^2 d^{-1} for the caprock aquifer, equation (1). Specific yield of the upper limestone unit ranges from 0.1 to 0.2 and aquifer thickness determined from well logs in southern Oahu varies between 20 m and 80 m (ref. 10), yielding hydraulic conductivity between 170 and 1,300 m d^{-1} (respectively; Supplementary Fig. S2a). Assuming average values of specific yield (0.15) and aquifer thickness (50 m), the unique hydraulic-conductivity estimate would be 400 m d^{-1}. All conductivity estimates are consistent with previous estimates of the coral- and reef-limestone deposits in the upper caprock[8,11].

Measured mean water levels are divided into wet and dry years to account for annual variations (Fig. 3b). The calculated groundwater table, equation (2), was fitted to measured data from both wet and dry years. The root mean square errors between measured and calculated water levels of the wet and dry years are 0.145 and 0.066 m (respectively). To simplify the assessment, the average water table

[1]Water Resources Research Center, University of Hawaii, 2540 Dole Street, Honolulu, Hawaii 96822, USA, [2]SOEST/Geology and Geophysics, University of Hawaii, 1680 East-West Road, Honolulu, Hawaii 96822, USA. *e-mail: kolja@hawaii.edu.

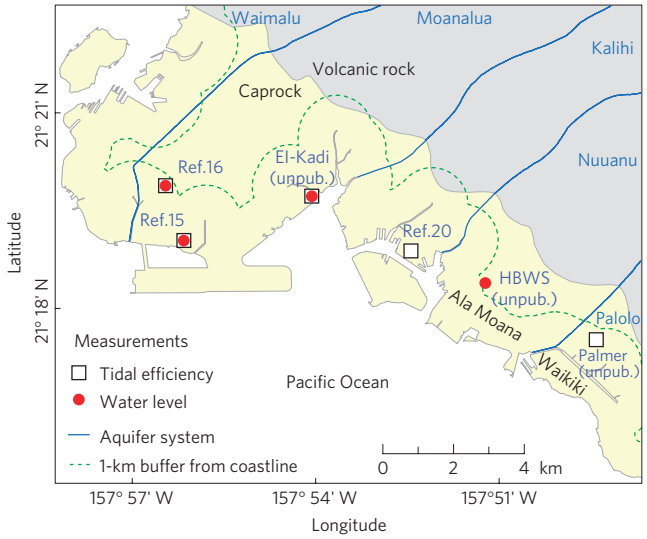

Figure 2 | Map of the study area of southern Oahu, Hawaii, surficial geology, aquifer-system boundaries and locations of tidal-efficiency and groundwater-level measurements.

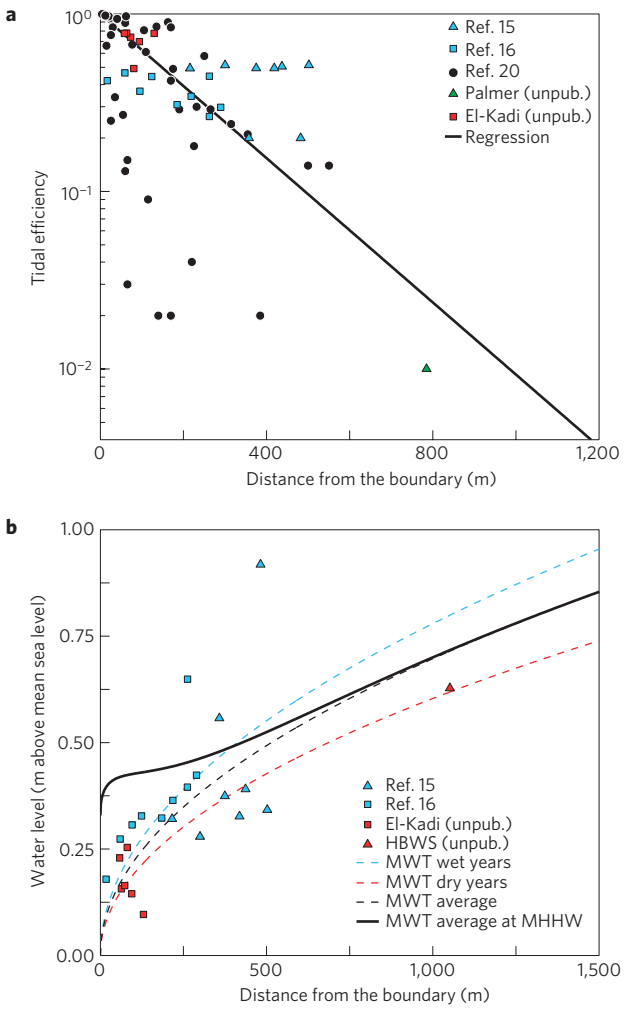

Figure 3 | Measurements in the southern Oahu aquifer. a, Tidal amplitude attenuation with distance from the coastline. **b**, Mean groundwater-level measurements and estimated mean water table (MWT).

of wet and dry years is used. To obtain an independent check on the estimated groundwater level, and assuming a recharge rate over the caprock of 2.0 $m^2\ d^{-1}$, the leakage from the basalt to the caprock aquifer is 2.0 $m^2\ d^{-1}$, which is consistent with previously reported values[11,12]. To disregard individual tidal fluctuations, the offset between mean higher high water (MHHW) and current mean sea level is multiplied by the tidal efficiency with distance from the boundary and added to the mean water table to yield an estimated steady-state groundwater table at MHHW (Fig. 3b).

The estimated water table at MHHW is projected throughout the Honolulu and east Pearl Harbor caprock aquifer as a function of distance from the shoreline (Supplementary Fig. S1), which is the best regional estimate in the absence of further observations. Model uncertainty and sensitivity are addressed in the Supplementary Information. Flooding mostly occurs within a 1-km wide coastal zone along the shoreline, and a SLR of 0.33 m has little effect on inundation, but a 0.66 m SLR, and a more pronounced 1.0 m SLR, reveals widespread groundwater inundation of the land surface (Fig. 4b) that is much greater than marine inundation (Fig. 4a). The flooded area including groundwater inundation is twice the area of marine inundation alone for the 0.33-m SLR scenario (Table 1). For a 0.66 m SLR, the portion of groundwater inundation to total flooded area increases to 69%, and it is 58% for a 1 m SLR.

At first, groundwater inundation will occur infrequently, usually when high tide is coinciding with heavy rainfall. In the chronology implied by semi-empirical models[13], areas lying within 0.33 m of modern MHHW are especially vulnerable to the impacts of SLR by mid-century, whereas those lying between 0.66 and 1 m are vulnerable in the latter half of the century. Throughout the study area, flooded regions occupy 0.5% within the heavily urbanized 1-km buffer for the 0.33-m SLR scenario (Table 1). Under 0.66-m SLR, inundated areas increase to 2.5% of the total area, and for 1-m SLR 5.8 km^2 or 10% is flooded. The ratio of inundated areas to total area in individual aquifer systems is similar to the total numbers. However, it is noteworthy that the inundation in Waikiki (Palolo aquifer) and Ala Moana (Nuuanu aquifer) is higher with 13.5 and 19% of the area within the 1-km buffer under a 1-m SLR (respectively). This is consequential for businesses and tourism, and also for residents inland of Waikiki.

The vertical uncertainty for the estimated flooded areas is ±0.35 m (Supplementary Information), indicating that areas inundated by 0.66 m SLR, for example, could be the areas now presented by the 0.33-m or the 1.0-m SLR scenarios. Limitations also include the one-dimensional assessment of aquifer properties and water levels. Higher confidence in projecting groundwater inundation can be achieved with more continuous groundwater measurements throughout the study area and higher resolution topographic data.

Figure 4b and Supplementary Fig. S3b depict flooded regions due to groundwater inundation at higher sea levels. This can be used to plan for SLR adaption in: the design of infrastructure such as hospitals, urban drainage, wastewater treatment, and roadways; cases where public health and safety are at risk; and in the management of natural ecosystems and resources. Along the shoreline, impacts will also include beach erosion and marine inundation from wave overtopping with increased frequency and magnitude. At inland areas, impacts will include reduced infiltration and drainage, and saltwater intrusion. Urban drainage systems in coastal areas rely on the ability to drain surface runoff into the ocean. As sea level rises, groundwater inundation will prevent infiltration and drainage. It is likely that future urban settings will be characterized by standing pools of brackish water, maximized at high tide. This may affect traffic, walkways, and any movement in urbanized coastal areas. Eventually, runoff from rainstorms will encounter few drainage options. Travel, commerce, and emergency services may be impacted and groundwater

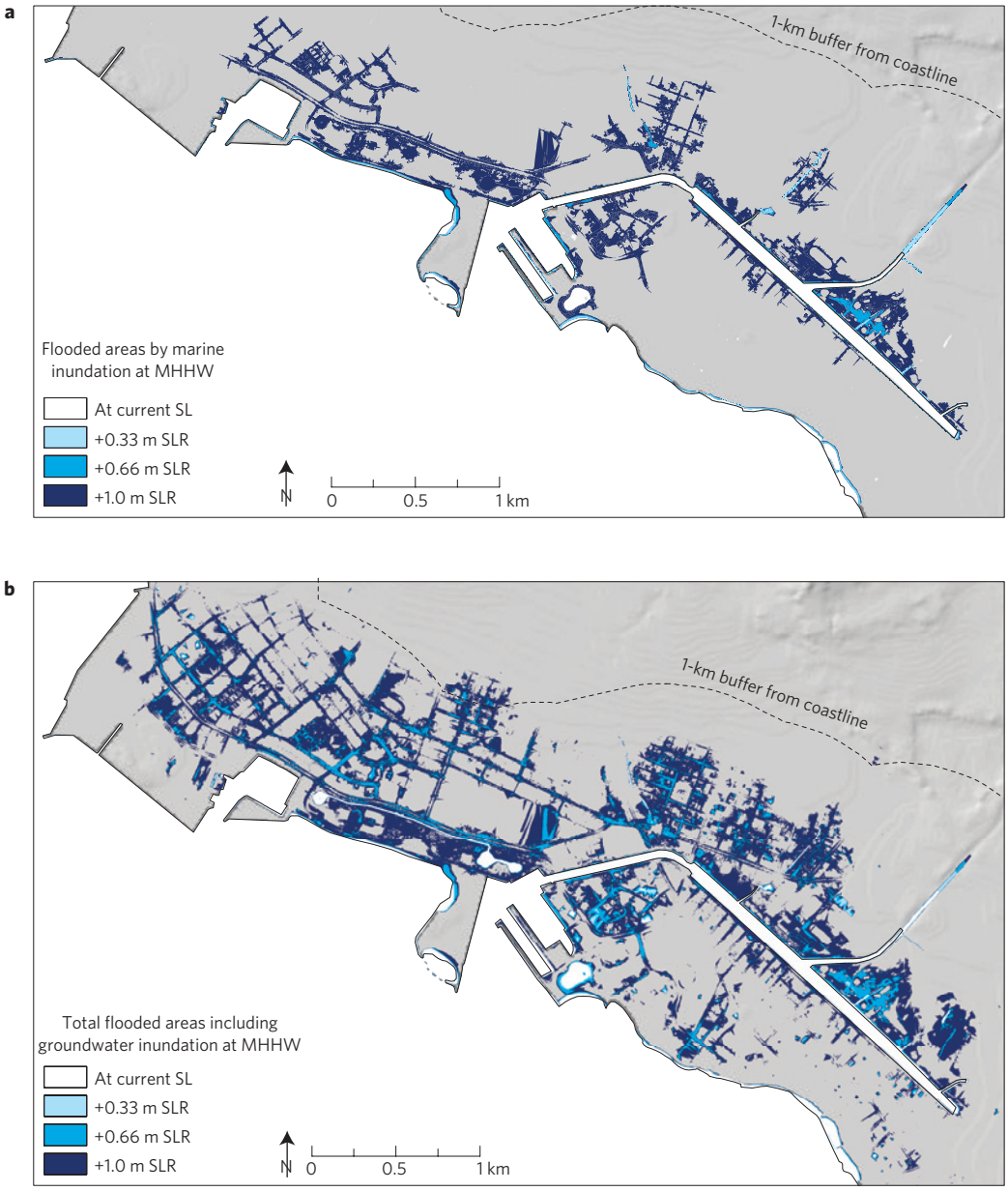

Figure 4 | Inundation at MHHW under sea-level rise in the Honolulu caprock aquifer, Oahu, Hawaii. a, Marine inundation and **b**, total inundated areas including groundwater inundation.

Table 1 | Total flooded areas by groundwater inundation and marine inundation within 1 km of the southern Oahu coastline and percentage of flooded area by groundwater inundation over total flooded area for several SLR scenarios.

Aquifer	Total flooded area (km^2)			Total flooded area, in percentage of area in 1-km buffer			Flooded portion by groundwater inundation, in percentage of total flooded area		
	Sea-level rise (m)								
	0.33	0.66	1.0	0.33	0.66	1.0	0.33	0.66	1.0
Palolo	0.04	0.23	1.09	0.51	2.8	13.5	48	69	54
Nuuanu	0.02	0.21	1.32	0.23	3.0	19.0	42	88	66
Kalihi	0.06	0.17	0.52	0.59	1.8	5.4	48	36	55
Moanalua	0.11	0.53	1.97	0.62	2.9	10.7	68	76	63
Waimalu	0.08	0.31	0.87	0.54	2.1	5.8	33	64	42
Total	0.31	1.44	5.76	0.53	2.5	9.9	51	69	58

inundation may change the character of the land surface in ways that work against public health and safety. Furthermore, increased soil saturation may lead to a series of geotechnical and slope-stability issues. For example, rising aquifer salinity leads to corrosion of subsurface structures, including water and sewer pipes[6]. A higher water table may also cause increased evaporation and groundwater discharge.

Groundwater withdrawals from wells in the study area are used for irrigation of landscaping and golf courses, small-scale agriculture, and water for cooling purposes. Although a rising sea level, seawater intrusion, and higher concentrations of brackish water in the coastal aquifer imply a degradation of water quality in places that use fresh groundwater for drinking-water purposes, the effects of SLR on caprock water resources on Oahu are minimal because potable water is not withdrawn from the caprock aquifer. Developed coastal aquifers are generally more vulnerable to groundwater extraction than to SLR (ref. 14), and because withdrawals lower water tables, it reduces the likelihood for them to rise and cause flooding. Thus, groundwater withdrawals can be used to mitigate the effects of a rising water table, even if it means pumping brackish water to avoid inundation. As groundwater inundation is largely unrecognized but potentially relevant, we recommend rigorous planning in affected areas. It is important to have a detailed understanding of the spatial distribution of the coastal groundwater level and temporal resolution of the processes that control changes in water-table height, and it is therefore essential to monitor groundwater levels continuously throughout the coastal zone.

Methods

Groundwater levels in the coastal zone oscillate with the ocean surface; thus, mean water levels of continuous measurements provide more meaningful data than discrete measurements. Measured mean water levels in the Honolulu and Pearl Harbor caprock aquifer include observations in the Moanalua aquifer near Hickam Airforce Base in 2005 (refs 15,16), at the Greyline Terminal near the Honolulu International Airport in 2002 (El-Kadi, unpublished), and one discrete measurement at the Beretania pumping station in 2011 by the Honolulu Board of Water Supply (HBWS, unpublished), where tidal influence is negligible (Fig. 2). Water levels measured in 2005 correspond to a relatively wet year, and those measured in 2002 and 2011 correspond to relatively dry years[9].

Tidal efficiency is the ratio of amplitude variation in a well compared to ocean-tide amplitude. It is conveniently used to estimate hydraulic properties, such as hydraulic conductivity and storage parameters of coastal aquifers, and is applicable to unconfined aquifers when tidal amplitudes are small in relation to aquifer thickness[17,18]. The relation of amplitude attenuation with distance from the boundary provides a regional aquifer-diffusivity estimate, D ($m^2\,d^{-1}$), which yields a hydraulic-conductivity estimate, K ($m\,d^{-1}$), assuming plausible values for aquifer thickness, b (m), and specific yield, S_y (dimensionless)[19]:

$$D = \frac{Kb}{S_y} = \frac{x^2\pi}{(\ln A)^2\tau} \quad (1)$$

where x is distance to the coastal boundary (m), A is tidal efficiency (dimensionless), and τ is the period of the oscillation (d). Owing to higher correlation and thus higher confidence in the tidal efficiency, time lags are not considered in the analysis. The increase in aquifer thickness due to a sloping water table is small compared with the total aquifer thickness and effects are neglected. Tidal efficiencies were measured in the Moanalua aquifer near Hickam Airforce Base[15,16], at the Greyline Terminal (El-Kadi, unpublished), in the Kalihi aquifer[20], and in the Willows Pools (Palmer, unpublished; Fig. 2).

Simplifying the observations to one dimension by assuming homogeneity of caprock-aquifer properties throughout the Honolulu and Pearl Harbor area allow estimates of a generalized water table at steady-state conditions, h (m relative to mean sea level), using the equation of Glover[4]:

$$h = \sqrt{\frac{2(\rho_s - \rho_f)qx}{\rho_s K}} \quad (2)$$

where ρ_s is the saltwater density ($kg\,m^{-3}$), ρ_f is the freshwater density ($kg\,m^{-3}$), and q is the freshwater flow per unit length of shoreline ($m^2\,d^{-1}$). Density of salt- and freshwater is assumed 1,025 and 1,000 $kg\,m^{-3}$ (respectively). Flow through the caprock aquifer includes surficial recharge and leakage from the basalt to the caprock aquifer. Recharge over the east Pearl Harbor caprock is estimated as 2 $m^2\,d^{-1}$ (ref. 12) and estimates of leakage rates to the caprock aquifer are similar[11,21]. The regional caprock hydraulic conductivity is estimated from tidal-amplitude attenuation, equation (1), and the water-table height with distance from the shoreline is estimated by varying the freshwater flux in equation (2) and minimizing the root mean square error between calculated and measured water levels. Hydraulic-conductivity estimates of the upper limestone unit of the caprock from tidal analyses on the southwest coast of Oahu range from 8 to 8,700 $m\,d^{-1}$ (ref. 21). Oki[8] simulated that unit with a horizontal hydraulic conductivity of 760 $m\,d^{-1}$. A sensitivity analysis shows the effects of the parameters affecting the calculated water table (Supplementary Information).

Areas where the problem of groundwater inundation is likely to develop can be characterized by digital elevation models (DEM) derived from airborne LiDAR datasets. The National Geospatial-Intelligence Agency, among others, has collected LiDAR data for much of the Hawaiian Islands. The DEM of southern Oahu has a horizontal resolution of 1 m. A map of areas vulnerable to groundwater inundation was obtained by subtracting the DEM from the estimated regional water table and adding estimates of SLR in 0.33-m increments up to a worst-case scenario of 1 m by end of the century. The linear increase in water-table height with SLR is applicable in flux-controlled systems where the seaward groundwater flux is maintained[22], for example, in freshwater-lens aquifers underlain by saltwater that is directly connected to ocean fluctuations (Fig. 1). Water tables may not rise linearly with SLR; the coastline will shift and changes in recharge or discharge are likely with a changing climate and a rising water table. These processes are transient and may lead to a nonlinear response of the water table to SLR.

Marine inundation is assessed by isolating DEM cells that are hydrologically connected to the ocean or adjacent flooded cells using the 8-side approach[23], and including areas connected through underground drainage channels, which are not apparent from the DEM. Areas vulnerable to marine inundation are obtained by adding estimates of SLR to MHHW in 0.33-m increments up to 1 m. Consequently, the part of the total flooded area that is not marine inundation is considered groundwater inundation.

Received 29 June 2012; accepted 20 September 2012; published online 11 November 2012

References

1. Rignot, E., Velicogna, I., van den Broeke, M. R., Monaghan, A. & Lenaerts, J. Acceleration of the contribution of the Greenland and Antarctic ice sheets to sea level rise. *Geophys. Res. Lett.* **38,** LO5503 (2011).
2. National Research Council *Sea Level Rise for the Coasts of California, Oregon, and Washington: Past, Present, and Future* (Board on Earth Sciences and Resources, Ocean Studies Board, 2012).
3. Nicholls, R. J. Planning for the impacts of sea level rise. *Oceanography* **24,** 144–157 (2011).
4. Glover, R. E. The pattern of freshwater flow in a coastal aquifer. *J. Geophys. Res.* **64,** 457–459 (1959).
5. Rotzoll, K. & El-Kadi, A. I. Estimating hydraulic properties of coastal aquifers using wave setup. *J. Hydrol.* **353,** 201–213 (2008).
6. Bjerklie, D. M., Mullaney, J. R., Stone, J. R., Skinner, B. J. & Ramlow, M. A. *Preliminary Investigation of the Effects of Sea-level Rise on Groundwater Levels in New Haven, Connecticut*. USGS OFR 2012–1025 (USGS, 2012).
7. Nicholls, R. J. Coastal megacities and climate change. *Geo J.* **37,** 369–379 (1995).
8. Oki, D. S. *Numerical Simulation of the Effects of Low-permeability Valley-fill Barriers and the Redistribution of Ground-water Withdrawals in the Pearl Harbor Area, Oahu, Hawaii*. USGS SIR 2005–5253 (USGS, 2005).
9. Rotzoll, K., Oki, D. S. & El-Kadi, A. I. Changes of freshwater-lens thickness in basaltic islands aquifers overlain by thick coastal sediments. *Hydrogeol. J.* **18,** 1425–1436 (2010).
10. Stearns, H. T. & Vaksvik, K. N. Geology and ground-water resources of the island of Oahu, Hawaii. *Hawaii Div. Hydrogr. Bull.* **1** (1935).
11. Oki, D. S., Souza, W. R., Bolke, E. L. & Bauer, G. R. Numerical analysis of the hydrogeologic controls in a layered coastal aquifer system, Oahu, Hawaii, USA. *Hydrogeol. J.* **6,** 243–263 (1998).
12. Rotzoll, K. *Numerical Simulation of Flow in Deep Open Boreholes in a Coastal Freshwater Lens, Pearl Harbor Aquifer, O'ahu, Hawai'i*. USGS SIR 2012–5009 (USGS, 2012).
13. Rahmstorf, S., Perrette, M. & Vermeer, M. Testing the robustness of semi-empirical sea level projections. *Clim. Dynam.* **39,** 861–875 (2012).
14. Ferguson, G. & Gleeson, T. Vulnerability of coastal aquifers to groundwater use and climate change. *Nature Clim. Change* **2,** 342–345 (2012).
15. CH2M HILL Tidal Study Data Report, *Site SS11 South/AMC Ramp Area, Hickam Air Force Base, Oahu, Hawaii*. Air Force Center for Environmental Excellence—Pacific Division Contract F41624-03-D-8595, Task Order 332 (United States Air Force, 2006).
16. CH2M HILL Tidal Study Data Report, *Chlorinated VOCs plume area at site LF05, Hickam Air Force Base, Oahu, Hawaii*. Air Force Center for Environmental Excellence—Pacific Division Contract F41624-03-D-8595, Task Order 8 (United States Air Force, 2006).

17. Rotzoll, K., El-Kadi, A. I. & Gingerich, S. B. Analysis of an unconfined aquifer subject to asynchronous dual-tide propagation. *Ground Water* **46,** 239–250 (2008).
18. Merritt, M. L. *Estimating Hydraulic Properties of the Floridan Aquifer System by Analysis of Earth-tide, Ocean-tide, and Barometric Effects, Collier and Hendry Counties, Florida*. USGS WRI Report 2003–4267 (USGS, 2004).
19. Jacob, C. E. in *Engineering Hydraulics* (ed. Rouse, H.) 321–386 (John Wiley, 1950).
20. CH2M HILL *Tidal Study Data Report, Iwilei Unit, Oahu Hawaii* Iwilei District Participating Parties, LLC (CH2M HILL, 2004).
21. Camp Dresser and McKee Inc. *Groundwater modeling study: Review of existing data, Ewa marina project*. Report to Haseko (Ewa), Inc, Honolulu, HI (1993).
22. Werner, A. D. & Simmons, C. T. Impact of sea-level rise on sea water intrusion in coastal aquifers. *Ground Water* **47,** 197–204 (2009).
23. Cooper, H. M., Chen, Q., Fletcher, C. H. & Barbee, M. Assessing vulnerability due to sea-level rise in Maui, Hawaii using LiDAR remote sensing and GIS. *Climatic Change* http://dx.doi.org/10.1007/s10584-012-0510-9 (2012).

Acknowledgements

We appreciate discussions with Delwyn Oki (USGS). This study was funded by grants from the U.S. Department of the Interior, Pacific Islands Climate Change Cooperative and the National Oceanographic and Atmospheric Administration-Coastal Storms Program.

Author contributions

K.R. and C.H.F. designed the research; K.R. carried out the research and analyses, and developed the inundation maps; K.R. and C.H.F. wrote the paper.

Additional information

Supplementary information is available in the online version of the paper. Reprints and permissions information is available online at www.nature.com/reprints. Correspondence and requests for materials should be addressed to K.R.

Competing financial interests

The authors declare no competing financial interests.